Journal of Chromatography, 640 (1993) 79–96
Elsevier Science Publishers B.V., Amsterdam

CHROMSYMP. 2643

Review

Pulsed amperometric detection of carbohydrates, amines and sulfur species in ion chromatography —the current state of research

Dennis C. Johnson*, David Dobberpuhl, Richard Roberts and Peter Vandeberg

Department of Chemistry, Iowa State University, Ames, IA 50011 (USA)

ABSTRACT

A review is given of so-called pulsed amperometric detection at Au and Pt electrodes. Of greatest interest is the application of pulsed amperometric detection for polar aliphatic compounds not easily detected by conventional photometric or fluorometric techniques. The anodic detection mechanisms are electrocatalytic in nature under the control of potential-dependent surface states. Oxidations of carbohydrates at Au electrodes in alkaline media occur in a potential region where a submonolayer of adsorbed hydroxyl radicals ($^{\bullet}OH_{ads}$) is formed and speculation is offered on the role of this species in the anodic mechanisms. Very little anodic signal is obtained at Au electrodes for low-molecular-mass *n*-alcohols; however, a large response is obtained from oxidation of the alcohol moiety of *n*-alkanolamines. This is attributed to the beneficial effect of adsorption via the amine moiety with the result that the residence time of the molecules at the electrode surface is increased to give a high probability for ultimate oxidation. Amines and sulfur compounds with non-bonded electrons on the N and S atom, respectively, are adsorbed at Au electrodes and are oxidatively desorbed concomitantly with formation of inert surface oxide (AuO). The simultaneous formation of surface oxide produces a large background signal in pulsed amperometric detection. Hence, a modification of the pulsed waveform is described whose application is called integrated pulsed amperometric detection. Applications are shown for pulsed amperometric detection and integrated pulsed amperometric detection in ion chromatography to illustrate strengths of these combined technologies.

CONTENTS

* Corresponding author.

0021-9673/93/$24.00

1. CONCEPTS OF ELECTROCATALYTIC DETECTION

1.1. Introduction

The development of ion chromatography (IC) in both the suppressed and non-suppressed forms has relied heavily on electrochemical detection [1–4]. At its inception, IC utilized conductance detection (CD) and, because of its simplicity and reliability for both inorganic and organic ions, CD continues as the most common detection technique in IC. Potentiometric detection also has been used in IC. Applications have included complexing agents at Cu electrodes, and halides and pseudo-halides at Ag electrodes. More recently, much interest has been directed to amperometric detection in IC as a result of successful separations of organic compounds [5–8].

This review is focused on anodic detection of aliphatic compounds based on electrocatalytic mechanisms at Pt and Au electrodes under the control of multi-step potential–time (E–t) waveforms [5–8]. Applications of these detection mechanisms have included simple alcohols, polyalcohols, carbohydrates, amines and some sulfur compounds. A description of the voltammetric basis of this detection technology is given here with examples of chromatographic applications.

1.2. Background

Many polar aromatic compounds are detected in aqueous media by oxidation at conventional anodes (*e.g.*, Au, Pt and C in its various forms) using constant (d.c.) applied potentials. Included are phenol, aminophenols and catecholamines, and numerous applications have appeared for liquid chromatography (LC) [9]. In contrast, d.c. detection is consistently ineffective for aliphatic alcohols and amines at these same electrodes. The reactivity of aromatic compounds is believed to benefit from conjugated bonding which stabilizes free-radical oxidation products and, thereby, lowers the activation barrier. However, a similar mechanism does not exist in aliphatic compounds and their oxidations are typically slow or non-existent at inert electrodes.

Absence of π-bonding in aliphatic compounds also has the consequence of low sensitivity for photometric (UV–Vis) detection. Hence, development of detection procedures for polar aliphatic compounds separated by various forms of LC has represented a major challenge to analytical chemistry. Many ad-

vances have been reported in the use of pre-injection and post-column chemical derivatizations to generate photometrically as well as electrochemically active adducts [10,11]. Nevertheless, the authors believe there will always be preference for the simplicity of direct detection, whenever available with sufficient sensitivity.

1.3. Electrocatalytic oxidation mechanisms

A premise of the detection strategy reviewed here is that activation barriers for oxidation of polar aliphatic compounds can be decreased at clean Au and Pt electrodes which have unsaturated surface d-orbitals. These surfaces stabilize free-radical oxidation products by adsorption and, thereby, can promote faradaic reactions of numerous polar aliphatic compounds. However, a consequence of adsorption can be extensive fouling of surfaces by accumulated detection products. Hence, historical consensus of non-reactivity for many aliphatic compounds at Au and Pt electrodes is actually a consequence of the high but short-lived activity of these electrode surfaces.

Faradaic processes are described as *electrocatalytic* when the electrode surface interacts beneficially within the reaction mechanisms. A characteristic of electrocatalytic mechanisms is that the voltammetric response of members within a family of compounds is controlled primarily by the potential dependence of the requisite catalytic surface state. Hence, mixtures of compounds reacting by the same electrocatalytic mechanism cannot possibly be resolved on the basis of their voltammetric response. Therefore, the greatest analytical utility of electrocatalytic detection mechanisms is obtained when they are coupled with chromatographic systems to achieve *a priori* separations.

1.4. Renewal of electrode surface activity

A serious consequence of strong adsorption of organic molecules and free radicals on Au and Pt electrodes can be the attenuation of surface reactivity. However, these adsorbates are usually oxidatively desorbed quite efficiently by application of a large positive potential step to achieve anodic formation of surface oxides (AuO and PtO) [12,13]. A subsequent large negative potential step quickly achieves cathodic dissolution of the oxides to restore the native reactivity of the clean surfaces.

Large positive and/or negative potential pulses have long been used for activation of solid electrodes. Table 1 contains a brief historical review of the associated literature. Of greatest significance to this review are multi-step waveforms which alternate amperometric detection with surface cleaning and reactivation to achieve continuous monitoring of chromatographic effluents.

1.5. pH Requirements

The heterogeneous rate constants for electrocatalytic oxidations of polar aliphatic compounds at clean Au and Pt surfaces are generally observed to increase with increasing pH. This pH effect is undoubtedly the result of H^+ production in the anodic mechanisms. Nevertheless, the minimum pH for satisfactory analytical response is dependent on the choice of electrode material. For example, high sensitivity for anodic detection of carbohydrates at Au electrodes requires pH $\geqslant$ *ca.* 12, whereas detection at Pt electrodes is satisfactory even at pH <1. This dramatic difference in the minimal useful pH is attributed to the lower electronic occupancy of the surface d-orbitals at Pt and, therefore, a greater ability to promote reactions by stabilization of free-radical oxidation products. Nevertheless, Au electrodes are more popular than Pt. One reason is that dissolved O_2 contributes a cathodic response at Pt over the entire potential range useful for anodic detection, whereas careful selection of detection potential at Au can avoid serious O_2 interference.

1.6. Selection of chromatographic phases

The need for pH control in chromatographic applications of electrocatalytic anodic detections at Au and Pt electrodes can be achieved by post-column additions of an appropriate buffer solution. However, greatest convenience and economy is achieved whenever separation phases are available that are tolerant of the conditions of pH and ionic strength desired for optimum detector response. Hence, polymeric separation phases developed for IC are highly preferred over silica-based phases developed for reversed-phase LC because of their greater stability over an extended pH range.

TABLE 1

HISTORICAL OVERVIEW OF APPLICATIONS OF MULTISTEP POTENTIAL–TIME WAVEFORMS FOR THE CLEANING AND REACTIVATION OF SOLID ELECTRODE SURFACES

Pos. = Positive; neg. = negative; C = glassy carbon electrode.

Author(s)	Year	Electrode	Summary	Ref.
Hammett	1924	Pt	Pos. pulses applied for pretreatment of electrode prior to oxidation of H_2	14
Armstrong *et al.*	1934	Pt	Pos. pulses applied for pretreatment of electrode prior to reduction of O_2	15
Gilman	1963	Pt	Pos./neg. pulses applied for electrode pretreatment in study of oxidation of simple alcohols	16
Breiter	1963	Pt and others	Pos./neg. pulses applied for electrode pretreatment in study of methanol oxidation	17
Giner	1964	Pt	Pos./neg. pulses applied for electrode pretreatment in study of alcohol oxidation	18
Adams	1969	Pt and C	Application of pos./neg. pulses recommended as general procedure for pretreatment for solid electrodes	19
Clark *et al.*	1972	Pt	Pos./neg. pulses applied for reactivation of electrodes during oxidation of ethylene	20
MacDonald and Duke	1973	Pt	Pos./neg. pulses applied for reactivation of electrodes during oxidation of *p*-aminophenol	21
Fleet and Little	1974	C	Use of two-step waveform decreased rate of electrode fouling in flow-through cell	22
Stulik and Hora	1976	Pt	Pos./neg. pulses for periodic reactivation of electrode during cathodic detection of Fe^{3+} and Cu^{2+}	23
Van der Linden and Diekes	1980	C	Pos./neg. pulses recommended as general means of electrode pretreatment	24
Van Rooijen and Poppe	1981	C	Periodic application of square-wave pulse train for electrode reactivation	25
Ewing *et al.*	1981	C	Application of two-step waveform for pulse voltammetry at microelectrodes to decrease rate of electrode fouling	26
Hughes *et al.*	1981	Pt	Pos./neg. pulses used in a three-step waveform for anodic detection of simple alcohols	27
Hughes and Johnson	1983	Pt	Three-step waveform for anodic detection of carbohydrates following chromatographic separation	28
Edwards and Haak	1983	Au	Three-step waveform for anodic detection of carbohydrates following chromatographic separation	29
Polta and Johnson	1983	Pt	Three-step waveform for anodic detection of amino acids following chromatographic separation	30
Polta and Johnson	1986	Au	Three-step waveform for anodic detection of sulfur compounds	31
Neuburger and Johnson	1987	Pt and Au	Three-step waveform for pulsed voltammetric comparison of carbohydrate response	32
Neuburger and Johnson	1988	Au	Multi-step waveform for oxide-catalyzed detection with automatic background rejection	33
Chen *et al.*	1992	Pt	Three-step waveform for pulse voltammetry at microelectrode in intracellular fluid	34
LaCourse and Johnson	1992	Au	Automated optimization of three-step waveforms for carbohydrate detection	35

2. EXPERIMENTAL

Voltammetric data were obtained at rotated disk electrodes (RDEs) using Models MSR rotators and RDE4 potentiostats (Pine Instrument Co). Analog waveforms at slow scan rates (50–100 mV/s) were generated within the RDE4. Staircase waveforms were generated external to the RDE4 by an IBM-compatible PC using Asyst 2.0 software (Asyst Technologies). Studies with fast scans ($\gg$ 50 mV/s) used analog waveforms generated by a Model 175 programmer connected to a Model 173 potentiostat (EG&G Princeton Applied Research). Digital recording of electrode response was achieved using IBM-compatible PCs with Asyst software. Interface boards were the DT-2800 (Data Translation) or DAS-1602 (MetraByte).

Counter electrodes in all voltammetric studies were Pt wires separated from the test solutions by fritted-glass junctions. Reference electrodes were saturated calomel electrodes (SCEs) separated from the test solutions by fritted-glass junctions.

Solutions were prepared from reagent-grade chemicals (Fisher Scientific) with water that had been purified by passage through two D-45 demineralizing cartridges (Culligan) and further treatment in a Milli-Q system (Millipore). When desired, solutions were deaerated by dispersed N_2 and an inert atmosphere was maintained over the solutions.

Chromatographic data shown for sulfur compounds were obtained using a Model GPM-2 pump (Dionex). All other chromatographic data are reproduced from earlier publications and the associated experimental details can be found in the references cited.

3. RESIDUAL VOLTAMMETRIC RESPONSE OF ELECTRODES

A complete description of amperometric detection must begin with the voltammetric response observed in the absence of analyte for an electrode potential applied according to the triangular waveform in Fig. 1A. That response is discussed here for Au in alkaline media and Pt in acidic media.

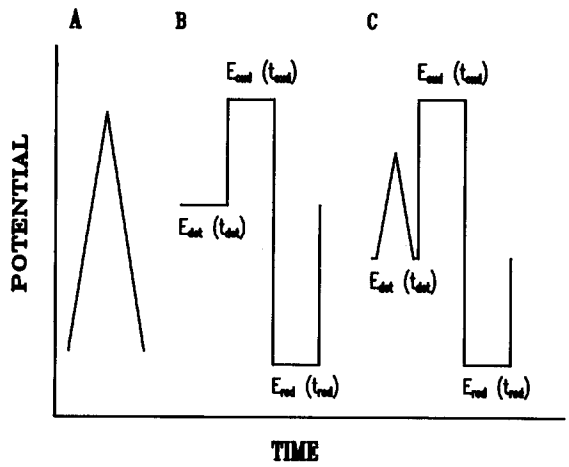

Fig. 1. Potential–time (E–t) waveforms. Curves: (A) voltammetric detection, (B) pulsed amperometric detection, (C) integrated pulsed amperometric detection. E_{det} = Detection potential; E_{red} = reduction potential; E_{oxd} = oxidation potential; t_{det} = detection period; t_{red} = reduction period; t_{oxd} = oxidation period.

3.1. Gold

Residual current–potential (i–E) curves obtained for a Au rotated disk electrode (RDE; 16.4 mm^2) in 0.1 M NaOH are shown in Fig. 2 for the absence (A and C) and presence (B) of dissolved O_2. The waveform (Fig. 1A) producing curves A and B was generated by analog instrumentation. Therefore, potential was a continuous function of time and elec-

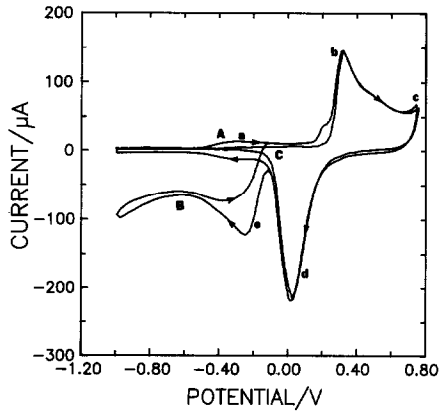

Fig. 2. Voltammetric response for a Au RDE in 0.10 M NaOH. Conditions: 400 rpm rotation, 500 mV/s scan. Solution: (A and C) deaerated, (B) aerated. Waveform generation (Fig. 1A): (A and B) analog, (C) digital. For a–e, see text.

trode current (i) was recorded as a continuous function of potential. Wave a, observed on the positive scan in the region *ca.* −0.6 to +0.1 V, is believed to correspond to anodic discharge of H_2O with formation of a submonolayer of adsorbed hydroxyl radicals ($^{\bullet}OH_{ads}$), frequently designated AuOH, perhaps at dislocated Au atoms or small atomic clusters. A monolayer of inert surface oxide (AuO) is formed during the positive scan for $E >$ *ca.* +0.2 V (wave b) and solvent breakdown with O_2 evolution occurs for $E >$ *ca.* +0.6 V (wave c). Evolution of O_2 and formation of AuO cease with scan reversal at +0.75 V and cathodic dissolution of AuO occurs in the region +0.2 to −0.1 V (peak d). Dissolved O_2, if present (curve B), is cathodically detected at $E <$ *ca.* −0.2 V (wave e).

Curve C was obtained using a waveform generated by digital instrumentation in which potential was advanced by 25-mV increments (ΔE) applied at 50-ms intervals (Δt). This so-called *staircase* waveform is a good approximation of the analog waveform when ΔE and Δt are very small. In obtaining curve C, current was sampled digitally after a 15-ms delay following each application of ΔE. Hence, contribution from double-layer charging is negligible. Also minimized are contributions from fast faradaic transformations of the electrode. Hence, there is almost no signal in curve C corresponding to wave a in curves A and B for anodic generation of $^{\bullet}OH_{ads}$. The remaining features of curve C are identical to curve A.

3.2. Platinum

Typically, Pt electrodes are chosen only when the sensitivity of Au electrodes is not sufficient. Specifically, this corresponds to detection of low-molecular-mass *n*-alcohols and glycols. These compounds can be detected with high sensitivity at Pt even in acidic media. Residual voltammetric curves obtained using a triangular analog waveform (Fig. 1A) are shown in Fig. 3 for a Pt RDE (16.4 mm^2) in 0.1 *M* $HClO_4$. Dissolved O_2 was present only for curve B. During the positive scan, a submonolayer of $^{\bullet}OH_{ads}$ is believed to form in the regions *ca.* +0.2 to +0.5 V (wave a), inert surface oxide (PtO) is generated at $E >$ *ca.* +0.5 V (wave b) and rapid discharge of H_2O with evolution of O_2 occurs for $E >$ *ca.* +1.2 V (wave c). Scan reversal at +1.3 V

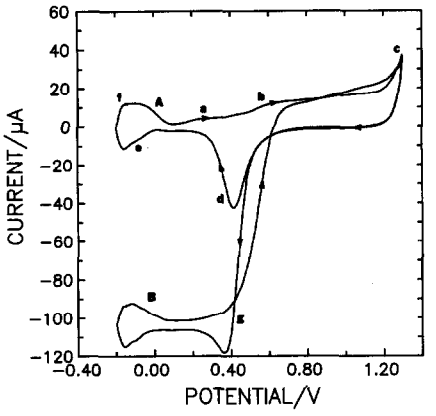

Fig. 3. Voltammetric response of a Pt RDE in 0.10 *M* NaOH. Conditions: 400 rpm, 50 mV/s. Solution: (A) deaerated, (B) aerated. Waveform generation (Fig. 1A): analog. For a–f, see text.

causes O_2 evolution and PtO formation to cease, and the current remains at virtually zero until cathodic dissolution of PtO occurs in the region +0.5 to +0.2 V (wave d). Continuation of the negative scan results in cathodic production of adsorbed hydrogen atoms ($^{\bullet}H_{ads}$) at $E <$ *ca.* 0.0 V (wave e) and evolution of H_2 at $E < -0.2$ V (not shown). Upon scan reversal at −0.2 V, anodic desorption of $^{\bullet}H_{ads}$ occurs in the region −0.2 to 0.0 V (wave f). Dissolved O_2, when present (curve B), is cathodically detected at $E <$ *ca.* +0.4 V (wave g).

4. DETECTION STRATEGIES

4.1. Reaction modes

There are two unique modes of anodic electrocatalytic detection that are available at Au and Pt electrodes [5,8,36]. These are described for Au in 0.1 *M* NaOH.

4.1.1. Mode I detection

This detection mode corresponds to anodic mechanisms that occur with production of a submonolayer of $^{\bullet}OH_{ads}$ but virtually no inert oxide (AuO), *i.e.*, *ca.* $-0.6 < E < +0.2$ V *vs.* SCE for Au in 0.1 *M* NaOH. The residual current in this potential region is small and decays quickly to a negligible value during a brief delay period following a step to the detection potential. Applications of

mode I detection at Au have been in alkaline media for carbohydrates and polyalcohols [29,37–45], and *n*-alkanolamines [46]. Mode I detection at Pt electrodes has included carbohydrates and polyalcohols in alkaline media [28], and alcohols and glycols in acidic media [47].

4.1.2. Mode II detection

This detection mode corresponds to anodic mechanisms catalyzed by formation of inert surface oxide (AuO) for $E > +0.2$ V *vs.* SCE in 0.1 *M* NaOH. We conclude that the monolayer of $^{\bullet}OH_{ads}$ (AuOH) generated as an intermediate product in the production of AuO is the source of oxygen being transferred to the oxidation products of mode II detection mechanisms. Contributions to the analytical signal originate both from oxidation of adsorbed analyte and analyte being transported to the electrode surface simultaneously with AuO formation. Generally, the anodic response is quickly terminated with scan reversal when formation of AuO (and $^{\bullet}OH_{ads}$) ceases. Therefore, detection requires current measurement simultaneously with AuO formation and, hence, a large background signal can be obtained. A unique approach will be described to minimize problems originating from the background signal. Applications of mode II detection at Au have been in alkaline media for amines and amino acids [48], and some sulfur compounds [49,50].

4.2. Pulsed amperometric detection

The amperometric detection of carbohydrates and polyalcohols in alkaline media based on mode I mechanisms can be managed successfully by multistep *E–t* waveforms of the type illustrated by Fig. 1B. The detection potential (E_{det}) is chosen to give the maximum desired response and the faradaic signal is sampled by digital integration for a short time period (t_{int}) following a brief delay (t_{del}) in the detection period (*i.e.*, $t_{det} = t_{del} + t_{int}$). Subsequently, the electrode is oxidatively cleaned by a positive step to $E_{oxd} \gg E_{det}$ (t_{oxd}) and then reductively reactivated by a negative step to $E_{red} \ll E_{det}$ (t_{red}) prior to repetition of the waveform. Amperometric detection under control of multi-step waveforms is called pulsed amperometric detection. Optimization of pulsed amperometric detection waveforms has been discussed [35,42,43,51].

The value of t_{int} in pulsed amperometric detection is chosen to maximize the signal-to-noise ratio (*S/N*). A major noise component is sinusoidal and is correlated with the 60-Hz line frequency. Hence, it is common to integrate the electrode current over an integral number (*m*) of 60-Hz cycles (*i.e.*, $t_{int} = 16.7m$ ms) [52]. Accordingly, a large *m* value results in increased signal strength without a significant increase in noise. Typically, $m = 12$ (*i.e.*, $t_{int} = 200$ ms). Signal output in pulsed amperometric detection can be the integral of current ($\int i\partial t$) or the average current ($\int i\partial t/t_{int}$).

4.3. Integrated pulsed amperometric detection

A large baseline signal from formation of surface oxide is obtained when the pulsed amperometric detection waveform in Fig. 1B is applied for mode II detection mechanisms. Furthermore, the baseline signal is commonly observed to drift to more anodic values, especially for new for freshly polished electrodes, because of the slow increase in electrode area as a consequence of surface reconstruction from the repeated formation/dissolution cycles for the surface oxide.

The problem of baseline offset and drift in mode II detections is diminished significantly by use of the waveform in Fig. 1C [33]. In this waveform, the electrode current is integrated during the entirety of a rapid cyclic scan of E_{det} within the detection period. Oxidative detection of analyte occurs concomitantly with oxide formation during the positive scan and the oxide is reduced during the subsequent negative scan. Because the charge for oxide reduction (negative scan) is approximately equal but with opposite polarity to the charge for oxide formation (positive scan), the signal on the electronic integrator at the conclusion of t_{det} can be virtually zero. Furthermore, the background signal is relatively unaffected by gradual changes in electrode area and less time is required for baseline stabilization during start-up of IC–integrated pulsed amperometric detection systems [33]. This detection strategy is referred to as IPAD.

The following guidelines apply for application of IPAD at Au electrodes in 0.1 *M* NaOH [33,53]: (i) the cyclic scan of E_{det} must begin and end at a value for which the electrode is free of surface oxide, *i.e.*, $\leqslant$ *ca.* -0.1 V *vs.* SCE; (ii) the positive scan of E_{det}

should not extend to values > *ca.* +0.6 V *vs.* SCE corresponding to solvent breakdown and O_2 evolution ; (iii) if dissolved O_2 is present, the negative scan of E_{det} should not extend to values < −0.1 V *vs.* SCE corresponding to detection of O_2. Incorrect choice of the negative scan limit for E_{det} can result in a substantial baseline when dissolved O_2 is present. When possible, it is preferable to deaerate the mobile phase with dispersed He and to use O_2-impermeable connective tubing for assembly of IC–IPAD systems.

5. CARBOHYDRATES AND POLYALCOHOLS

5.1. Voltammetric response at Au electrodes

The mode I response of carbohydrates is represented in Fig. 4 by that for glucose (curve B) obtained using the analog *E–t* waveform (Fig. 1A) at a Au RDE (16.4 mm^2) in 0.1 *M* NaOH. Curve A shows the residual response for Au in this media. During the positive scan, oxidation of the aldehyde moiety of glucose to produce the gluconate anion (number of electrons in reaction, n = 2 equiv./mol) occurs for E > *ca.* −0.6 V (wave a) coincident with formation of the submonolayer of $^{\bullet}OH_{ads}$ [54]. The heterogeneous rate constant for this oxidation is fast and the anodic current at *ca.* −0.35 V in the plateau region is limited by the rate of convective-diffusional transport of glucose to the Au RDE surface. The $^{\bullet}OH_{ads}$ is believed to play an important role in anodic reactions that occur with transfer of oxygen from H_2O to the oxidation products [55]. Evidence for this is the observation that half-wave potentials ($E_{1/2}$) for numerous O-transfer reactions are virtually identical and coincident with the onset of wave a in the residual *i–E* curve. According to this mechanism, $^{\bullet}OH_{ads}$ generated by anodic discharge of H_2O is the intermediate form of oxygen to be transferred from H_2O to the oxidation product. It is also possible that an adsorption step in the oxidation mechanism for polyalcohols and carbohydrates is facilitated by the presence of $^{\bullet}OH_{ads}$.

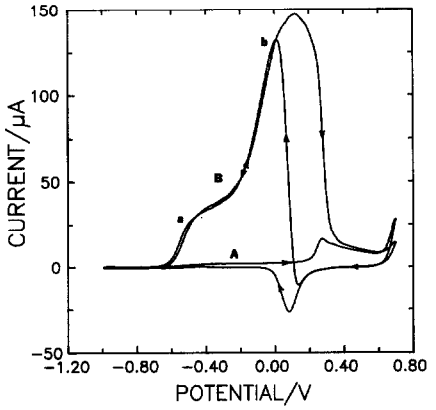

Fig. 4. Voltammetric response of glucose at an Au RDE in 0.10 *M* NaOH. Conditions: 400 rpm, 50 mV/s. Glucose (m*M*): (A) 0.0, (B) 0.5. For a and b, see text.

All carbohydrates (aldoses and ketoses) and polyalcohols produce a large anodic peak response at *ca.* +0.15 V similar to wave b for glucose in Fig. 4. The peak for glucose corresponds to an overall reaction with n approaching 10 equiv./mol for fluid velocities typical of flow-through detection cells [54]. This n value is consistent with an overall oxidation of glucose in alkaline media corresponding to oxidative cleavage of the C_1–C_2 and C_5–C_6 bonds with production of two moles of formate and one mole of dicarboxylate dianion. It is tentatively concluded that oxidations of all carbohydrates and polyalcohols proceed from the terminal carbons. Accordingly, mass sensitivity in pulsed amperometric detection is observed to decrease with increasing molecular mass.

It is significant that the anodic mode I response for glucose is sharply attenuated during the positive scan at E > +0.2 V (see Fig. 4). Whereas the Au surface would become fouled during d.c. detection at +0.15 V over an extended time period, the attenuation shown in Fig. 4 results from oxide formation and not from adsorption of detection products. Oxidation of glucose resumes on the negative scan almost immediately following the onset of cathodic dissolution of surface oxide at E < *ca.* +0.1 V. This behavior is true for all carbohydrates and polyalcohols. We interpret these results to indicate that mode I oxidation of carbohydrates and polyalcohols occurs only at highly reactive sites on the Au surface representing a small fraction of the total area (*i.e.*, <0.2). It is at these sites that oxide (AuO) is first produced during the positive scan and from which the oxide is first to be removed during the negative scan. This conclusion is supported by the observation that scan reversal at +0.30 V results in the return of the current to an anodic value on the

negative scan almost equal to the peak current at +0.15 V observed on the preceding positive scan. These observations indicate that the catalytic sites for oxidation of carbohydrates and polyalcohols are those sites at which the submonolayer of $^{\bullet}OH_{ads}$ is formed during the positive scan for $E > -0.6$ V *vs.* SCE. Furthermore, we conclude these sites correspond to Au atoms with low coordination number in the metal surface, *i.e.*, dislocated atoms, and, possibly, small clusters of Au atoms.

5.2. Chromatographic separations

Carbohydrates and polyalcohols are weakly acidic with $pK_a > 12$ [56]. Hence, separations are easily achieved from alkaline mobile phase (pH > 12) using low-capacity anion-exchange columns [38,42, 57]. These alkaline media are also appropriate for pulsed amperometric detection by the mode I mechanism at Au electrodes. Retention time is inversely correlated with pK_a value and increases dramatically with increasing molecular mass. Retention time can be decreased conveniently by addition of acetate ion (OAc^-). Olechno *et al.* [38] demonstrated the separation of 43 components of a partially hydrolyzed sample of corn starch within a 35-min period using a linear solvent gradient form 0.1 *M* NaOH to 0.1 *M* NaOH + 0.6 *M* NaOAc.

Shown in Fig. 5 is the separation of a mixture of polyalcohols, monosaccharides and small oligosaccharides [5]. Initially, the small polyalcohols are eluted isocratically with 50 m*M* NaOH (0–6 min). Next, the elution of xylose, fructose, sucrose and maltose is achieved by a linear solvent gradient that brings the mobile phase to 75 m*M* NaOH + 250 m*M* NaOAc (6–15 min). Finally, members of the oligosaccharides, ranging from maltotriaose to maltoheptaose (degree of polymerization, DP = 3–7), are eluted isocratically by 75 m*M* NaOH + 250 m*M* NaOAc (15–21 min). The detection limit for glucose is well below 1 ng ($S/N = 3$) with a linear response over more than four decades in concentration.

Larew and co-workers [58,59] considered the challenge of quantification of chromatographic peaks for glucose polymers with DP = 2–7. A short (1.5 cm) reactor column containing immobilized glucoamylase was placed between the chromatographic column and the detector to achieve conversion of polyglucose compounds to the equivalent amount of glucose. For 100% conversion to glucose, a single glucose calibration curve suffices for peak quantification. Conversion efficiency of the short reactor column was *ca.* >95% for DP = 4–7 but <90% for DP = 2 (maltose). Hence, longer reactor columns are recommended to achieve uniformly quantitative conversion of all oligosaccharides. The reactor column was refrigerated when not in use and conversion efficiency did not decrease during a 1-year period of use.

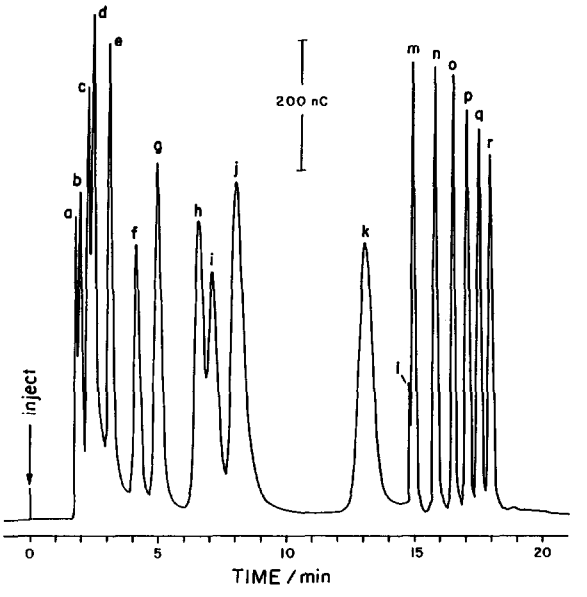

Fig. 5. Separation of carbohydrate mixture. Pulsed amperometric detection (mode I) at Au; Ag/AgCl reference; $E_{det} = +0.10$ V ($t_{det} = 610$ ms, $t_{del} = 400$ ms, $t_{int} = 200$ ms); $E_{oxd} = +0.80$ V ($t_{oxd} = 120$ ms); $E_{red} = -0.60$ V ($t_{red} = 200$ ms). Column: Dionex AS-6 Carbopac. Solvents: (A) 100 m*M* NaOH, (B) 50 m*M* NaOH + 0.5 *M* NaOAc, (C) H_2O. Elution: isocratic (0–6 min) with A–C (50:50); linear gradient (6–15 min) to A–B (50:50); isocratic (15–21 min) with A–B (50:50). Post-column addition: 0.4 *M* NaOH. Peaks: a = inositol; b = xylitol; c = sorbitol; d = mannitol; e = fucose; f = rhamnose; g = arabinose; h = glucose; i = xylose; j = fructose; k = sucrose; l = unknown; m = maltose; n = maltotriose; o = maltotetraose; p = maltopentaose; q = maltohexaose; r = maltopheptaose. From ref. 5 by permission from the American Chemical Society.

Anodic response of sugar amines can be based either on detection of the carbohydrate moiety (mode I) or the amine group (mode II). However, mode I detection yields greater sensitivity.

6. SIMPLE ALCOHOLS AND GLYCOLS

6.1. Voltammetric response at Pt electrodes

The mode I response of low-molecular-mass *n*-alcohols and glycols at Pt in acidic media is adequately represented by the *i–E* curve in Fig. 6 for ethylene glycol. During the positive scan, a peak response is observed at *ca.* +0.4 V corresponding to formation of a submonolayer of $^{\bullet}OH_{ads}$ on Pt. The anodic signal is sharply attenuated by formation of surface oxide (PtO) at $E > +0.5$ V. Cathodic dissolution of the surface oxide during the negative scan allows resumption of the oxidation of ethylene glycol and the current swings to a net anodic value in the region *ca.* +0.3 to +0.1 V.

6.2. Chromatography

Whereas simple *n*-alcohols are volatile and their separations and quantitative determinations can easily be achieved by gas chromatography (GC), glycols are sufficiently polar so that they are not readily determined by GC without *a priori* derivatization. Furthermore, the absence of conjugated bonding in these compounds has greatly restricted the use of photometric detection in the development of LC separations for their quantitative determinations.

Simple alcohols and glycols are easily detected by pulsed amperometric detection at Pt electrodes based on electrocatalytic mechanisms (mode I). Fig. 7 shows results for 13 alcohols and glycols separated by ion exclusion chromatography using an anion-exchange column with 0.050 *M* $HClO_4$ as the mobile phase [60]. This is a prime example of the utility of IC columns for separation of polar nonionic organic compounds. Detection limits for ethylene glycol by this method are typically *ca.* 10 ppb (w/w) ($S/N = 3$).

Results are shown in Fig. 8 for 13 alcohols separated by a mixed-mode IC column using a linear acetonitrile gradient [60]. Post-column addition of NaOH brought the chromatographic effluent to an alkaline pH to facilitate pulsed amperometric detection (mode I) at a Au electrode. The detection sensitivity for these compounds was diminished somewhat as a result of the competitive adsorption of acetonitrile at the catalytic reaction sites of the electrode.

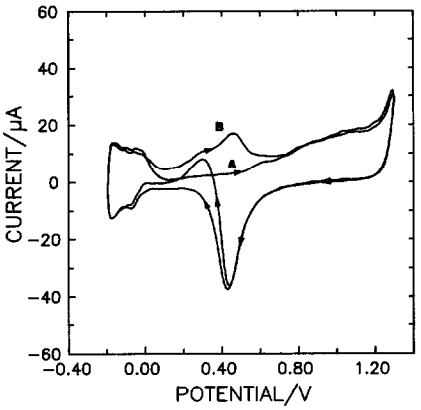

Fig. 6. Voltammetric response of ethylene glycol at a Pt RDE in 0.10 *M* $HClO_4$. Conditions: 400 rpm, 50 mV/s. Ethylene glycol (m*M*): (A) 0.0, (B) 0.5.

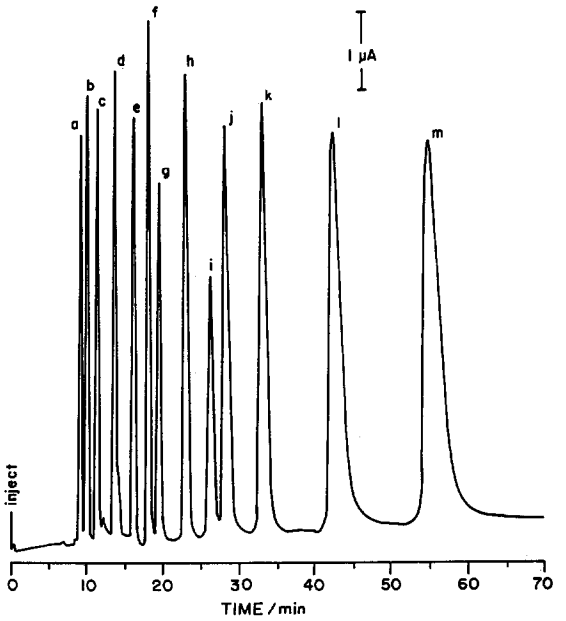

Fig. 7. Separation of alcohol mixture. Pulsed amperometric detection (mode I) at Pt; Ag/AgCl reference; $E_{det} = +0.30$ V (t_{det} = 300 ms, t_{del} = 280 ms, t_{int} = *ca.* 20 ms); $E_{oxd} = +1.40$ V (t_{oxd} = 120 ms); $E_{red} = -0.40$ V (t_{red} = 420 ms). Column: Dionex AS-1. Elution: isocratic, 50 m*M* $HClO_4$. Sample: 50 μl. Peaks: a = adonitol, 45 ppm; b = erythritol, 36 ppm; c = glycerol, 9 ppm; d = ethylene glycol, 10 ppm; e = methanol, 30 ppm; f = ethanol, 45 ppm; g = 2-propanol, 177 ppm; h = 1-propanol, 202 ppm; i = 2-butanol, 202 ppm; j = 2-methyl-1-propanol, 120 ppm; k = 1-butanol, 122 ppm; l = 3-methyl-1-butanol, 364 ppm; m = 1-pentanol, 365 ppm. From ref. 60 by permission from the American Chemical Society.

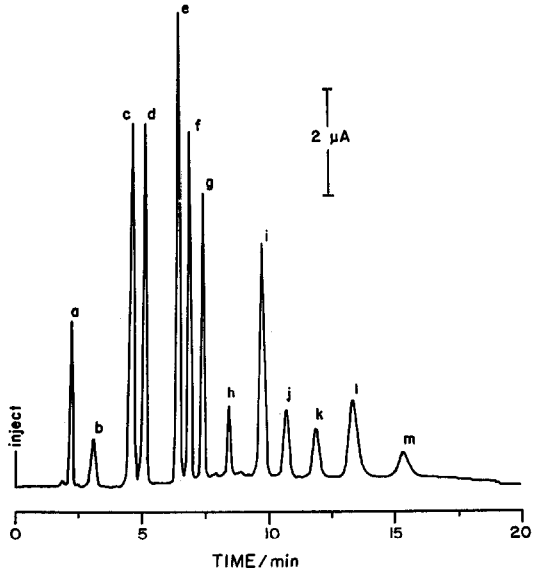

Fig. 8. Separation of alcohol mixture. Pulsed amperometric detection (mode I) at Au; Ag/AgCl reference; E_{det} = +0.10 V (t_{det} = 720 ms, t_{del} = 520 ms, t_{int} = *ca.* 200 ms); E_{oxd} = +1.00 V (t_{oxd} = 120 ms); E_{red} = −0.80 V (t_{red} = 300 ms). Column: Dionex OmniPAC PCX-500. Elution: gradient, 18–85.5% acetonitrile in water. Post-column addition: 0.3 *M* NaOH. Sample: 50 μl. Peaks: a = ethanol, 1840 ppm; b = 1-propanol, 460 ppm; c = 2-methyl-2-propen-1-ol, 46 ppm; d = cyclopentanol, 460 ppm; e = phenylmethanol, 69 ppm; f = 1-phenylethanol, 115 ppm; g = 3-phenyl-1-propanol, 115 ppm; h = 2-ethyl-1-hexanol, 460 ppm; i = 1-decanol, 460 ppm; j = 1-undecanol, 920 ppm; k = 1-dodecanol, 920 ppm; l = 1-tridecanol, 920 ppm; m = 1-tetradecanol, 920 ppm. From ref. 60 by permission from the American Chemical Society.

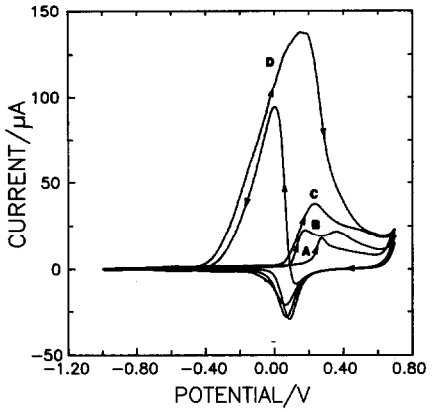

Fig. 9. Voltammetric response of amines at Au RDE in 0.10 *M* NaOH. Conditions: 400 rpm, 50 mV/s. Curves: (A) residual, (B) 0.5 m*M* glycine, (C) 0.5 m*M* ethylamine, (D) 0.5 m*M* ethanolamine.

7. ALKANOLAMINES AND AMINO ACIDS

7.1. Voltammetric response at Au electrodes

Amines can be detected by anodic oxidation at Au electrodes in alkaline media [46,61,62]. This response is illustrated in Fig. 9 by *i–E* curves for ethylamine (curve B), glycine (curve C) and ethanolamine (curve D), in comparison with the residual response for Au (curve A). Oxidation of amines that are adsorbed and being transported to the electrode occurs by the mode II mechanism in the region +0.1 to +0.6 V (positive scan) concomitantly with formation of surface oxide. Oxidation terminates with cessation of oxide formation as the result of scan reversal at +0.7 V. Products of amine oxidation have not yet been identified.

A unique response is observed for *n*-alkanolamines, as illustrated by curve D for ethanolamine (Fig. 9). The large peak response at *ca.* +0.15 V is characteristic of the oxidation of terminal alcohol groups in polyalcohols and carbohydrates (mode I). Hence, this peak for ethanolamine is attributed to oxidation of the $-CH_2OH$ moiety with production of the glycinate anion (n = 4 equiv./mol) [62]. The remarkable aspect of this observation is the fact that the anodic response for ethanol is very small at Au in 0.1 *M* NaOH. The large reactivity of the $-CH_2OH$ group in ethanolamine is attributed to the effect of adsorption of the N atom in the amine moiety with the consequence of retention of the neutral molecule at the electrode surface. Hence, even though the inherent rate constant is small for oxidation of $-CH_2OH$, the increased residence time at the electrode surface results in ultimate oxidation. The anionic oxidation product in this alkaline media is hydrophilic and, therefore, is rapidly desorbed to allow the adsorption site to be recycled in the electrocatalytic mechanism. This mechanism is sufficiently rapid to cause the peak response at +0.15 V to be virtually limited by the rate of mass transport. This mechanism is believed to apply for all *n*-alkanolamines.

7.2. Chromatography of alkanolamines

Alkanolamines are used extensively in chemical industry as emulsifying agents and corrosion inhibitors. They lack natural chromophores and fluorophores for photometric and fluorometric detection, and, furthermore, their high polarity virtually excludes quantitative determination by GC.

The separation of a mixture of linear and branched alkanolamines by reversed-phase paired-ion chromatography is shown in Fig. 10 with pulsed amperometric detection (mode I) at a Au electrode [46]. The mobile phase contained acetonitrile and sodium dodecyl sulfonate, as the ion-pairing agent. The peaks for monoethanolamine and triethanolamine are well resolved; however, monoethanolamine and diethylamine are co-eluted. The requirement of alkalinity for pulsed amperometric detection was achieved by post-column addition of NaOH. The detection limit (S/N = 3) for ethanolamine by this method is *ca.* 40 ppb (*i.e.*, 8 ng/200 μl sample) with a linear response to 10 ppm.

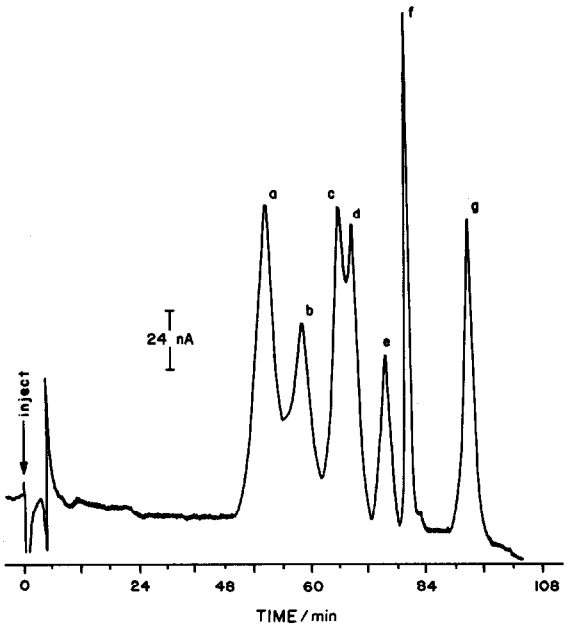

Fig. 10. Separation of alkanolamines. Pulsed amperometric detection (mode I) at Au; Ag/AgCl reference; E_{det} = +0.20 V *vs.* SCE (t_{del} = 280 ms, t_{int} = 17 ms, t_{det} = 300 ms), E_{oxd} = +1.00 V *vs.* SCE (t_{oxd} = 400 ms), E_{red} = −0.40 V *vs.* SCE (t_{red} = 350 ms). Column: Hamilton PRP-1 C_{18}. Solvents: (A) 0.75 m*M* dodecanesulfonate in acetonitrile–water (15:85), (B) 0.75 m*M* dodecanesulfonate and 10 m*M* $NaNO_3$ in acetonitrile–water (15:85). Elution: isocratic (0–50 min), 100% A; linear ramp (50–70 min) to A–B (90:10); linear ramp (70–71 min) to 100% B; isocratic (>71 min), 100% B. Post-column addition: 0.3 *M* NaOH. Sample: 200 μl. Peaks: a = 2-amino-1-ethanol, 3 ppm; b = 4-amino-1-butanol, 4 ppm; c = 5-amino-1-pentanol, 4 ppm; d = 2-amino-1-butanol, 3 ppm; e = 6-amino-1-hexanol, 2 ppm; f = 2-amino-1-pentanol, 2 ppm; g = 2-amino-1-hexanol, 4 ppm. From ref. 46 by permission from the American Chemical Society.

7.3. Chromatography of amino acids

The majority of amino acids in biological materials have been perceived historically as being electroinactive [63,64]. Nevertheless, all amino acids can be detected directly by the mode II mechanism at Au electrodes in alkaline media (see curve C in Fig. 9).

Chromatographic results are shown in Fig. 11 for a mixture of 20 amino acids in a protein hydrolyzate [61]. This separation required the use of a complex pH gradient described in ref. 61. In spite of post-column addition of NaOH, small fluctuations of pH were evident in the detector cell. Changes in pH cause a shift in the onset potential for the anodic wave resulting from oxide formation (wave b in Fig. 1) by the amount −59 mV/pH. Hence, for an increase in pH, the baseline obtained for pulsed amperometric detection (mode II) increases anodically.

The use of IPAD decreases significantly the baseline fluctuation caused by changes in pH; however, optimum potential values for the IPAD waveform also shift with change in pH. To eliminate this problem, a glass-membrane, H^+-selective electrode was used as the potential reference in the detector cell in place of the conventional pH-independent reference electrode, *e.g.*, Ag/AgCl(s) electrode [65,66]. Because the pH dependence of the glass-membrane electrode is the same as that for the anodic processes at the Au electrode, the voltammetric response at Au obtained using this reference appears to be independent of pH. Hence, results in Fig. 11 were obtained using a glass-membrane reference electrode.

Detection limits (S/N = 3) for essential amino acids by IPAD are *ca.* 3–5 pmol. It is especially significant that the sensitivity of IPAD is nearly the same for primary and secondary amino acids.

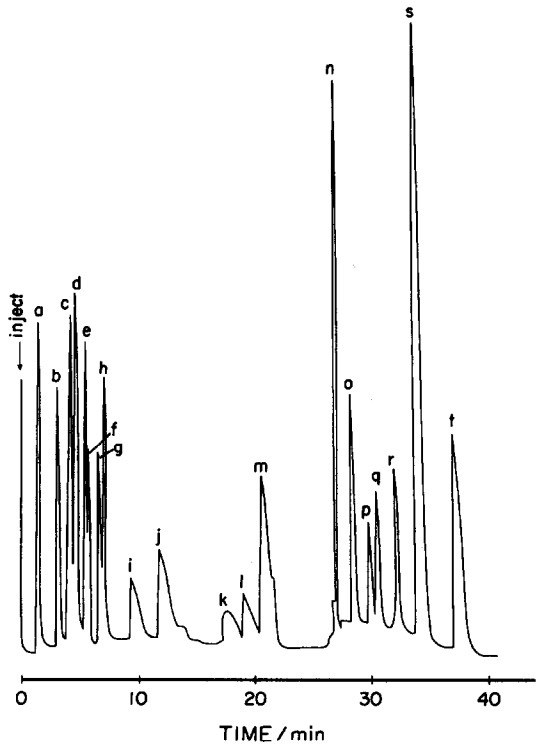

Fig. 11. Separation of amino acids in protein hydrolyzate. Detection: IPAD (mode II) at Au; glass-membrane reference; see waveform in Table III of ref. 48. Column: Dionex AS-8. Elution: gradient, see Table II of ref. 48. Sample: 50 μl. Peaks: a = arginine; b = lysine; c = glutamine; d = asparagine; e = threonine; f = alanine; g = glycine; h = serine; i = valine; j = proline; k = isoleucine; l = leucine; m = methionine; n = histidine; o = phenylalanine; p = glutamic acid; q = aspartic acid; r = cysteine; s = cystine; t = tyrosine. From ref. 48 by permission from the American Chemical Society.

8. SULFUR COMPOUNDS

8.1. Voltammetric response at Au electrodes

Numerous sulfur compounds are detected by mode II mechanisms at Au and Pt [31,50]. Detected are compounds having at least one non-bonded pair of electrons on the S atom. Examples include thioalcohols, thiophenes, thiocarbamates and organic thiophosphates. Sulfones and sulfonic acid derivatives are not detected.

The voltammetric response of thiourea is shown in Fig. 12 (curve B) obtained at a Au RDE (0.20 cm^2) in 0.1 *M* NaOH. The residual response is

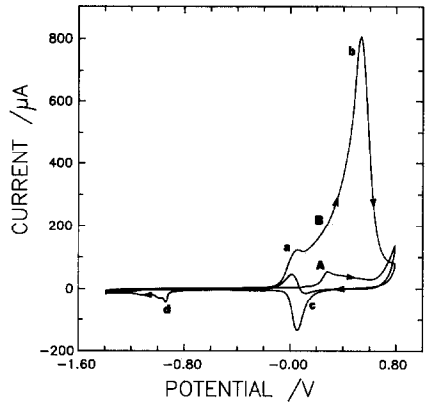

Fig. 12. Voltammetric response of thiourea at Au RDE in 0.10 *M* NaOH. Conditions: 1000 rpm, 100 mV/s. Curves: (A) residual, (B) 1.0 *M* thiourea. For a–d, see text.

shown by curve A [67]. Wave a starting at *ca.* −0.1 V (positive scan) occurs just prior to the onset of AuO formation and is attributed to the one-electron oxidation of the S atom with subsequent dimerization of the product to form formamidine disulfide [67,68]. Anodic peak b in the region *ca.* +0.2 to +0.7 V (positive scan) occurs concomitantly with oxide formation and corresponds to oxidative desorption of adsorbed formamidine disulfide as well as oxidation of thiourea transported to the electrode surface. Sulfate was identified as a major product of the anodic reactions contributing to peak b and these oxidation processes are concluded to occur by a catalytic O-transfer mechanism (mode II) [67]. The anodic O-transfer mechanism is severely attenuated for $E >$ *ca.* +0.5 V because the electrode surface becomes covered by the inert oxide layer (AuO).

With scan reversal at +0.8 V, further formation of oxide ceases and the current remains at zero until cathodic dissolution of AuO commences at *ca.* +0.1 V (peak c). Almost immediately, the net current swings to anodic values as a result of the oxidation of thiourea on the reduced portions of the electrode. Continued negative scan yields cathodic peaks d at $E < -0.9$ V. These peaks have been identified as resulting from cathodic desorption of S^0 formed at $E > +0.2$ V by incomplete oxidation of thiourea without oxygen transfer. If the negative scan is reversed at values > -0.9 V, S^0 accumulates with repeated cyclic scans to produce a visible film which causes severe attenuation of wave a and peak

b (positive scan). Conversely, if the negative scan is reversed at values < *ca.* −1.0 V, the electrode surface is cathodically cleaned of adsorbed S^0 within each consecutive cyclic scan, and wave a and peak b are large and reproducible [67].

It is apparent from Figs. 9 and 12 that both amines and sulfur compounds are detected concomitantly with oxide formation (mode II) at Au electrodes. There are situations in which selective detection of S compounds is desired without interference from the presence of amines, *e.g.*, chromatographic determination of cysteine, cystine and/or methionine in the presence of other amino acids. Fig. 13 compares the voltammetric response for 0.005 m*M* cysteine (curve B) and 0.5 m*M* glycine (curve C) at a Au RDE in 0.1 *M* $HClO_4$; the residual curve for Au is shown by curve A. Clearly, under these acidic conditions, the sensitivity for cysteine detection far exceeds that for glycine. Addition of 10% acetonitrile results in virtual elimination of the glycine signal. This occurs because acetonitrile is adsorbed on Au more strongly than amines in acidic media and blocks the electrocatalytic mechanism for anodic detection. Presence of the acetonitrile has virtually no effect on the detection of the more strongly adsorbed cysteine.

8.2. Chromatography

Chromatographic results using PAD (mode II) are shown in Fig. 14 for a beer sample spiked with 1 ppm ethylenethiourea (ETU). No sample clean-up was employed and separation was by a Dionex MPIC-NS1 column (20 cm) using 0.1 *M* NaOH as the mobile phase. The ETU is well resolved from the other beer components. The detection limit (S/N = 3) for ETU by this method is *ca.* 5 ppb.

Chromatographic results are shown in Fig. 15 for a mixture of 10 μM cysteine, methionine and cystine containing 1 m*M* alanine, glycine, serine and threo-

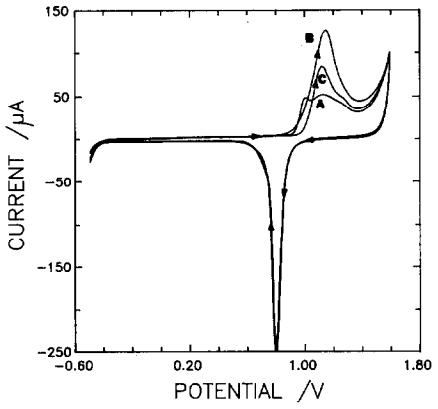

Fig. 13. Comparison of voltammetric response of cysteine and glycine at Au RDE in 0.10 *M* $HClO_4$. Conditions: 1000 rpm, 100 mV/s. Curves: (A) residual, (B) 0.005 m*M* cysteine, (C) 0.5 m*M* glycine.

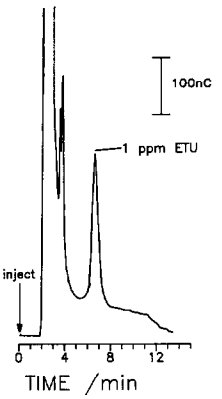

Fig. 14. Separation of 1 ppm ethylenethiourea (ETU) from other components of beer. Pulsed amperometric detection (mode II) at Au; Ag/AgCl reference; E_{det} = +0.50 V (t_{del} = 440 ms, t_{int} = 100 ms, t_{det} = 540 ms), E_{oxd} = +0.80 V (t_{oxd} = 60 ms), E_{red} = −1.30 V (t_{red} = 300 ms). Column: Dionex MPIC-NS1. Elution: isocratic, 100 m*M* NaOH, 1.0 ml/min. Sample: 50 μl.

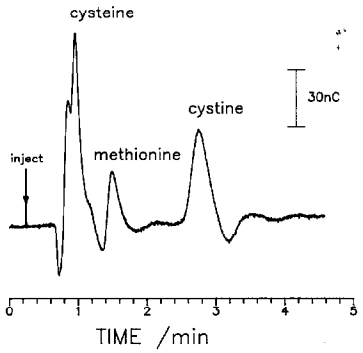

Fig. 15. Separation of 10 μM cysteine, methionine and cystine in the presence of 1 m*M* alanine, glycine, serine and threonine. Pulsed amperometric detection (mode II) at Au; Ag/AgCl reference; E_{det} = +1.60 V (t_{del} = 250 ms, t_{int} = 50 ms, t_{det} = 300 ms), E_{oxd} = +2.00 V (t_{oxd} = 30 ms), E_{red} = −0.50 V (t_{red} = 120 ms). Column: Dionex OmniPAC PCX-500 guard (5 mm length). Elution: isocratic, 0.5 *M* phosphate buffer–acetonitrile (95:5) (pH 1.6), 0.8 ml/min.

nine. A Dionex OmniPAC-PCX-500 guard column (5 mm) was used with 0.5 *M* phosphate buffer–acetonitrile (95:5) (pH 1.6) and pulsed amperometric detection (mode II) at a Au electrode in the acidic effluent. Under these conditions, peaks are obtained only for the S-containing amino acids.

9. FUTURE DEVELOPMENTS

9.1. Faster waveforms

Typical applications of pulsed amperometric detection and IPAD using mode I and II reaction mechanisms have utilized waveform frequencies in the range *ca.* 0.5 to 1 Hz for maximum *S/N*. However, recent improvements to column efficiencies and separation velocities, and the development of capillary columns, are providing motivation for the use of higher waveform frequencies to guarantee acceptable correlation between apparent and actual peak shapes. Because of the essential role of oxide formation and dissolution in the maintenance of reactive Au and Pt surfaces, it is expected that the kinetics of these processes will be a significant factor when increasing the frequency of pulsed amperometric detection and IPAD waveforms [69].

Fig. 16 contains an instructive illustration of the effect of finite kinetics on the residual voltammetric response at a Au RDE (0.78 mm^2) in 0.1 *M* NaOH. The *i–E* curves were obtained using a triangular analog *E–t* waveform (Fig. 1A) with values of scan rate (ϕ) increasing from 0.2 to 200 V/s. The current response was recorded digitally so the curves are not distorted by the slow response of an analog recorder. The basis of this illustration is the fact that, for a linear potential scan, the potential axis is a linear time (*t*) axis. Hence, increases in ϕ can cause the *i–E* response for a slow electrode process to be shifted along the potential axis in the direction of longer *t*.

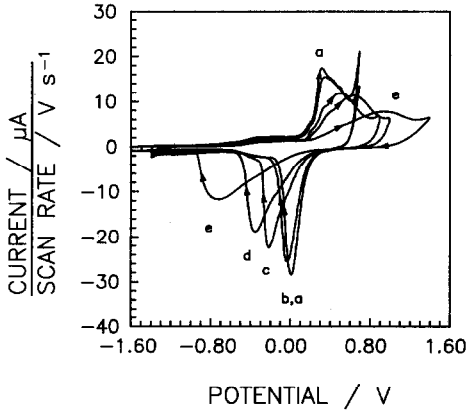

Fig. 16. Residual voltammetric response at a Au RDE in 0.10 *M* NaOH as a function of scan rate. Conditions: 1000 rpm. Scan rate (V/s): (a) 0.20, (b) 1.0, (c) 20, (d) 50, (e) 200.

During the positive scan at low ϕ values (≤ 1 V/s), the amount of oxide (AuO) formed at $E \geq$ *ca.* +0.2 V is virtually at an equilibrium value and, hence, the current for oxide formation is observed to be proportional to ϕ. Therefore, the current scale in Fig. 16 has been normalized with respect to ϕ. As a consequence, the normalized currents at *ca.* +0.2 V (positive scan) for ϕ = 0.2 and 1 V/s are virtually identical and no shift of the oxide-formation wave is observed. For $\phi > 1$ V/s, however, the anodic wave for oxide formation is shifted to higher potential values (longer *t*) and the maximum normalized current decreases as ϕ is increased. These observations are evidence that the oxide coverage lags behind its equilibrium value for fast scan rates (> 1 V/s) due to slow heterogeneous kinetics. The behavior of the cathodic peak (negative scan) corresponding to oxide dissolution is similar to that of the anodic wave for oxide formation, except that the peak shift is to more negative potentials. It is significant in Fig. 16 that the anodic wave for formation of $^{\bullet}OH_{ads}$ (wave a in Fig. 2) is not shifted over the range of ϕ values tested and this anodic process is concluded to be very fast.

The effect of increased ϕ on the voltammetric response of glucose at the Au RDE used in Fig. 16 is shown in Fig. 17. Clearly, the anodic wave for the aldehyde moiety ($E >$ *ca.* −0.6 V), a process believed to be promoted by formation of $^{\bullet}OH_{ads}$, is not shifted along the potential axis over the range of ϕ values tested. Likewise the anodic peak response at *ca.* +0.15 V, characteristic of all carbohydrates and polyalcohols, is not shifted as a consequence of increased ϕ. This is indicative of fast oxidation mechanisms.

In contrast to the response of carbohydrates and polyalcohols, the voltammetric response for amines and S compounds is dependent on formation of AuO. Hence, the anodic response for these compounds obtained using fast scan rates is shifted to higher potentials (longer *t*).

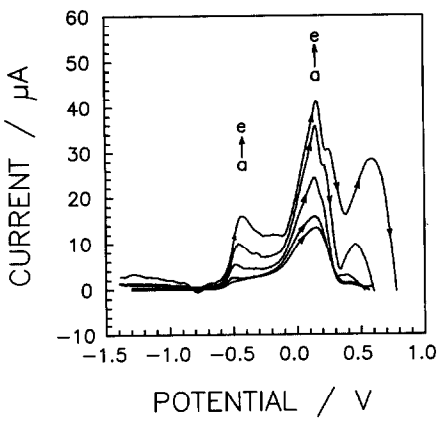

Fig. 17. Voltammetric response of 0.50 m*M* glucose at a Au RDE in 0.10 *M* NaOH as a function of scan rate. Conditions: 1000 rpm. Scan rate (V/s): (a) 0.20, (b) 1.0, (c) 5.0, (d) 20, (e) 50.

9.2. Voltammetric detection

The application of voltammetric detection in chromatographic separations has been reviewed [2,70]. The technique produces so-called chromatovoltammograms (*i–E–t* curves) which can be useful in the deconvolution of unresolved chromatographic peaks. Voltammetric detection under pulsed waveforms, including staircase waveforms, can be called pulsed voltammetric detection (PVD). PVD has been applied to capillary LC columns by Kennedy and Jorgenson [71].

Application of PVD to conventional LC columns was described by Owens *et al.* [72] using staircase Pt electrodes with cleaning and reactivation pulses between staircase scans. PVD with cleaning and reactivation pulses applied prior to each potential step can, in principle, be achieved by use of a pulsed amperometric detection waveform (Fig. 1B) in which E_{det} is varied according to a staircase waveform [32,34,35,52]. Accordingly, the electrode has a uniform activity for all potential values in the voltammetric response (*i–E*) curve. Whereas the use of small ΔE values in the staircase waveform increases voltammetric resolution, the time required for formation and dissolution of surface oxide with each cycle of the pulsed amperometric detection waveform necessitates a low rate of voltammetric scan. Hence, applications of this version of PVD in LC can be problematic because of the likelihood that the time to complete a scan of the staircase waveform will be greater than the chromatographic peak width.

The trend in chromatographic development is toward smaller injection volumes to improve chromatographic resolution with emphasis on highly diluted samples. These factors decrease the extent of electrode fouling and, as a result, it might not be necessary to apply a cleaning–reactivation cycle prior to each application of ΔE in the staircase waveform. We observe for dilute carbohydrate solutions (<1 m*M*) that electrode reactivity is maintained at a reproducible level provided the positive and negative scan limits in the staircase waveform are sufficient to permit the requisite processes of oxidation cleaning and reductive reactivation once within the execution of each waveform. The choice of scan limits for fast voltammetric waveforms must be made with consideration of the relatively slow kinetics for oxide formation and dissolution (see Fig. 16).

10. CONCLUSIONS

Numerous aliphatic compounds are detected with high sensitivity based on electrocatalytic oxidation mechanisms at Au and Pt electrodes under the control of multi-step potential–time waveforms. These waveforms alternate the processes of amperometric detection with oxidative cleaning and reductive reactivation of the electrodes to maintain high catalytic surface activity without the undesired effects of fouling as the result of accumulation of adsorbed detection products and/or solution impurities.

The high sensitivity and convenience of pulsed amperometric detection and IPAD at Au and Pt serve as further motivation to extend applications of IC columns for separations of non-ionic aliphatic compounds not detected by conductance and photometric measurements. A useful example is the ion-exclusion separation of alcohols and glycols.

The frequencies of pulsed amperometric detection and IPAD waveforms can be increased for applications to capillary columns, albeit not without some sacrifice to *S/N*. However, it is projected that the slow kinetics of oxide formation and dissolution at Au and Pt will limit the useful upper frequency to *ca.* 5–10 Hz.

Voltammetric resolution is not possible within classes of compounds whose anodic response is based on a common electrocatalytic mechanism. However, differences in voltammetric response for aldoses (reducing sugars) and all other carbohydrates might be useful in the deconvolution of poorly resolved chromatographic peaks. It is essential, however, that dissolved O_2 be maintained at a near-zero level if the voltammetric technique is to be applied for carbohydrates at low levels (<1 ppm).

11. ACKNOWLEDGEMENTS

This research is supported by grants form Dionex Corp., Sunnyvale, CA, USA, and the US National Science Foundation (grant CHE-8914700).

REFERENCES

1 D. T. Gjerde and J. S. Fritz, *Ion Chromatography*, Hüthig, Mamaroneck, NY, 2nd ed., 1987.
2 P. Jandik, P. R. Haddad and P. E. Sturrock, *CRC Crit. Rev. Anal. Chem.*, 20 (1988) 1.
3 H. Small, *J. Chromatogr.*, 546 (1991) 3.
4 R. D. Rocklin, *J. Chromatogr.*, 546 (1991) 175.
5 D. C. Johnson and W. R. LaCourse, *Anal. Chem.*, 62 (1990) 589A.
6 P. Luo, F. Zhang and R. P. Baldwin, *Anal. Chim. Acta*, 244 (1991) 169.
7 P. Luo, F. Zhang and R. P. Baldwin, *Anal. Chem.*, 63 (1991) 1702.
8 D. C. Johnson and W. R. LaCourse, *Electroanal.*, 4 (1992) 367.
9 R. E. Shoup, *Recent Reports on Liquid Chromatography–Electrochemistry*, Bioanalytical Systems Press, West Lafayette, IN, 1982. (*Note:* a recent listing can be obtained on database by contacting R.E.S.)
10 I. S. Krull (Editor), *Post-Column Reaction Detectors in HPLC*, Marcel Dekker, New York, 1986.
11 P. K. Dasgupta, *J. Chromatogr. Sci.*, 27 (1989) 422.
12 R. Woods, in A. J. Bard (Editor), *Electroanalytical Chemistry*, Vol. 9, Marcel Dekker, New York, 1976, p. 20.
13 S. Gilman, in A. J. Bard (Editor), *Electroanalytical Chemistry*, Vol. 2, Marcell Dekker, New York, 1967, p. 111.
14 L. P. Hammett, *J. Am. Chem. Soc.*, 46 (1924) 7.
15 G. Armstrong, F. R. Himsworth and J. A. V. Butler, *Proc. Roy. Soc. London (A)*, 143 (1934) 89.
16 S. Gilman, *J. Phys. Chem.*, 67 (1963) 78.
17 M. W. Breiter, *Electrochim. Acta*, 8 (1963) 973.
18 J. Giner, *Electrochim. Acta*, 9 (1964) 63.
19 R. N. Adams, *Electrochemistry at Solid Electrodes*, Marcel Dekker, New York, 1969, p. 206.
20 D. Clark, M. Fleishman and D. Pletcher, *J. Electroanal. Chem.*, 36 (1972) 137.
21 A. MacDonald and P. D. Duke, *J. Chromatogr.*, 83 (1973) 331.
22 B. Fleet and C. J. Little, *J. Chromatogr. Sci*, 12 (1974) 747.
23 W. Stulik and V. Hora, *J. Electroanal. Chem.*, 70 (1976) 253.
24 W. E. van der Linden and J. W. Diekes, *Anal. Chim. Acta*, 119 (1980) 1.
25 H. W. van Rooijen and H. Poppe, *Anal. Chim. Acta*, 130 (1981) 9.
26 A. G. Ewing, M. A. Dayton and R. M. Wightman, *Anal. Chem.*, 53 (1981) 1842.
27 S. Hughes, P. L. Meschi and D. C. Johnson, *Anal. Chim. Acta*, 132 (1981) 1.
28 S. Hughes and D. C. Johnson, *Anal. Chim. Acta*, 149 (1983) 1.
29 P. Edwards and K. K. Haak, *Am. Lab.*, April (1983) 28.
30 J. A. Polta and D. C. Johnson, *J. Liq. Chromatogr.*, 6 (1983) 1727.
31 T. Z. Polta and D. C. Johnson, *J. Electroanal. Chem.*, 209 (1986) 159.
32 G. C. Neuburger and D. C. Johnson, *Anal. Chem.*, 59 (1987) 203.
33 G. C. Neuburger and D. C. Johnson, *Anal. Chem.*, 60 (1988) 2288.
34 T. K. Chen, Y. Y. Lau, D. K. Y. Wong and A. G. Ewing, *Anal. Chem.*, 64 (1992) 1264.
35 W. R. LaCourse and D. C. Johnson, *Anal. Chem.*, 65 (1993) 50.
36 D. S. Austin-Harrison and D. C. Johnson, *Electroanal.*, 1 (1989) 189.
37 R. D. Rocklin and C. A. Pohl, *J. Liq. Chromatogr.*, 6 (1983) 1577.
38 J. Olechno, S. R. Carter, W. T. Edwards and D. G. Gillen, *Am. Biotech. Lab.*, 5 (1987) 38.
39 M. R. Hardy and R. R. Townsend, *Proc. Natl. Acad. Sci. U.S.A.*, 85 (1988) 3289.
40 M. R. Hardy, R. R. Townsend and Y. C. Lee, *Anal. Biochem.*, 170 (1988) 54.
41 R. R. Townsend, M. R. Hardy, O. Hindsgaul and Y. C. Lee, *Anal. Biochem.*, 174 (1988) 459.
42 W. R. LaCourse and D. C. Johnson, *Carbohydr. Res.*, 215 (1991) 159.
43 R. W. Andrews and R. M. King, *Anal. Chem.*, 62 (1990) 2130.
44 D. A. Martens and W. T. Frankenberger, Jr., *J. Chromatogr.*, 546 (1991) 297.
45 D. A. Roston and R. R. Rhinebarger, *J. Liq. Chromatogr.*, 13 (1991) 539.
46 W. R. LaCourse, W. A. Jackson and D. C. Johnson, *Anal. Chem.*, 61 (1989) 2466.
47 W. R. LaCourse, D. C. Johnson, M. A. Rey and R. W. Slingsby, *Anal. Chem.*, 63 (1991) 134.
48 L. E. Welch, W. R. LaCourse, D. A. Mead, Jr., D. C. Johnson and T. Hu, *Anal. Chem.*, 61 (1989) 555.
49 T. Z. Polta and D. C. Johnson, *Chromatogr. Forum*, 1 (1986) 37.
50 A. Ngoviwatchai and D. C. Johnson, *Anal. Chim. Acta*, 215 (1988) 1.
51 R. Rocklin, *Conductivity and Amperometry: Electrochemical Detection in Ion Chromatography*, Dionex, Sunnyvale, CA, 1991.
52 G. G. Neuburger and D. C. Johnson, *Anal. Chim. Acta*, 192 (1987) 205.

53 W. R. LaCourse and D. C. Johnson, in P. Jandik and R. M. Cassidy (Editors), *Advances in Ion Chromatography*, Vol. 2, Century International, Medfield, MA, 1990, p. 353.
54 L. A. Larew and D. C. Johnson, *J. Electroanal. Chem.*, 262 (1989) 167.
55 J. E. Vitt, L. A. Larew and D. C. Johnson, *Electroanal.*, 2 (1990) 21.
56 J. A. Rendleman, in H. S. Isbell (Editor), *Carbohydrates in Solution (Advances in Chemistry Series*, No. 117), American Chemical Society, Washington, DC, 1973, p. 51.
57 T. J. Paskach, H. P. Lieker, P. J. Reilley and K. Thielecke, *Carbohydr. Res.*, 215 (1991) 1.
58 L. A. Larew, D. A. Mead, Jr. and D. C. Johnson, *Anal. Chim. Acta*, 204 (1988) 43.
59 L. A. Larew and D. C. Johnson, *Anal. Chem.*, 60 (1988) 1867.
60 W. R. LaCourse, D. C. Johnson, M. A. Rey and R. W. Slingsby, *Anal. Chem.*, 63 (1991) 134.
61 L. E. Welch, W. R. LaCourse, D. A. Mead, Jr., D. C. Johnson and T. Hu, *Anal. Chem.*, 61 (1989) 555.
62 W. A. Jackson, W. R. LaCourse, D. A. Dobberpuhl and D. C. Johnson, *Electroanal.*, 3 (1991) 607.
63 M. Malfoy and J. A. Reynaud, *J. Electroanal. Chem.*, 114 (1980) 213.
64 H. M. Joseph and P. Davies, *Curr. Sep.*, 4 (1982) 62.
65 D. A. Mead, L. A. Larew and D. C. Johnson, in P. Jandik and R. M. Cassidy (Editors), *Advances in Ion Chromatography*, Century International, Franklin, MA, 1989, p. 13.
66 W. R. LaCourse, D. A. Mead and D. C. Johnson, *Anal. Chem.*, 62 (1990) 220.
67 P. J. Vandeberg, J. L. Kawagoe and D. C. Johnson, *Anal. Chim. Acta*, 260 (1992) 1.
68 V. A. Zakharov, I. M. Bessarabova, O. A. Songina and M. A. Timoshkin, *Elektrokhim.*, 7 (1971) 1215.
69 R. Roberts and D. C. Johnson, *Electroanal.*, 4 (1992) 741.
70 P. R. Haddad and P. Jandik, in J. G. Tarter (Editor), *Ion Chromatography*, Marcel Dekker, New York, 1987, p. 87.
71 R. T. Kennedy and J. W. Jorgenson, *Anal. Chem.*, 61 (1989) 436.
72 D. S. Owens, C. M. Johnson, P. E. Sturrock and A. Jaramillo, *Anal. Chim. Acta*, 197 (1987) 249.